On the extraction of linear and nonlinear physical parameters in nonideal diodes

V. Mikhelashvili, G. Eisenstein,[a] V. Garber, S. Fainleib, G. Bahir, D. Ritter, M. Orenstein, and A. Peer
Department of Electrical Engineering and Kidron Microelectronics Center, Technion—Israel Institute of Technology, Haifa 32000, Israel

(Received 17 September 1998; accepted for publication 26 January 1999)

We describe a parameter extraction technique for the simultaneous determination of physical parameters in nonideal Schottky barrier, *p-n* and *p-i-n* diodes. These include the ideality factor, saturation current, barrier height, and linear or nonlinear series, and parallel leakage resistances. The suggested technique which deals with the extraction of bias independent parameters makes use of the forward biased current–voltage ($I-V$) characteristics and the voltage-dependent differential slope curve $\alpha(V)=[d(\ln I)]/[d(\ln V)]$. The method allows (a) establishment of the current flow mechanisms at low and high bias levels, (b) extensive of the permissible ranges of determined parameters beyond what is possible in other published methods, and (c) to automation and computerization of the measurement processes. The method is verified experimentally using metal–semiconductor structures based on Si, InGaP, and HgCdTe as well as an InGaAs/InGaAsP multiple quantum well laser diode exemplifying a *p-n* junction. © *1999 American Institute of Physics.* [S0021-8979(99)04409-6]

I. INTRODUCTION

The forward biased current–voltage *(I–V)* characteristics of diodes of various types such as Schottky barrier diodes or *p-n* and *p-i-n* junctions can serve as the basis for the extraction of physical parameters: ideality factor (β), series (R_S), and leakage (R_P) resistances, and reverse saturation current (I_S), which determines the zero bias barrier height Φ_B provided that the Richardson constant is known. Parameter extraction requires a device model and a data analysis procedure. A large number of published techniques[1–10] describe solutions to this problem. Most publications deal with the case of bias independent parameters. This approach is in general sufficient for practical devices although some publications, for example,[9,10] address bias dependencies. However, this comes at the expense of severe complexity[9] and the inability to include the series resistance.[10] The advantages and limitations of the most common techniques are surveyed in Ref. 8 with the procedure introduced by Werner[5] standing out as the most reliable one. All published data analysis techniques have, however, some noticeable common disadvantages: (1) Two stages of graphical parameter extraction from the experimental $I-V$ characteristics are required. The first is used to determine the ideality factor and series resistance and the second to get the saturation current.[5,9] Alternatively,[1–4,6,7] the ideality factor and saturation current are found first followed by a determination of the series resistance. (2) A determination of the existence and establishment of the nature and magnitude of a leakage conductance requires an analysis of the reverse biased current–voltage characteristic which complicates the measurement.[5] (3) No published method accommodates a nonlinear series resistance. (4) All published parameter extraction techniques use many step-like graphical solutions and do not lend themselves to automation of the measurement processes, which is crucial for the selection of defective diodes in a mass production environment.

Here we propose and demonstrate a data analysis procedure that enables us to extract physical parameters and determine the details of the bias dependent carrier transport mechanism. The proposed technique makes use of the power exponent parameter α[11–14]

$$\alpha=\frac{d(\ln I)}{d(\ln V)}. \tag{1}$$

The technique we propose establishes first the nature of the carrier transport mechanisms at low and high voltage regimes in the presence of a possible parallel current path due to a shunt resistance. The current through the junction is allowed to have linear $I=V/R_S$ and nonlinear $I=V^n/A_0^n$ components (A_0 is a constant and n depends on the particular nonlinear mechanism taking place). Once the current mechanism is known, the procedure yields the diode parameters: β, R_S, A_0, R_P, and I_S or (Φ_B). The proposed technique assumes all parameters to be bias independent. While this is of course a limitation, it turns out not to be significant. This is evident from the experimental results discussed in Sec. V as well as in our recently published paper.[14] The bias dependence of the extracted parameters is further discussed in Sec. VI.

We compare the new technique to known alternatives and demonstrate, using simulated nonideal diode characteristics, its various advantages. The technique is shown to be superior specially for nonlinear diodes. Furthermore, the permissible ranges of the determined parameters are significantly wider than those obtainable with other methods[5] and the technique permits easy automation. Experimental verifi-

[a]Electronic mail: gad@ee.technion.ac.il

 © 1999 American Institute of Physics

cation was obtained using Si, InGaP, and HgCdTe Schottky diodes as well as an InGaAs/InGaAsP *p-n* junction of a multiple quantum well laser diode.

II. CONDUCTION PROCESS

The classical model of an ideal Schottky barrier diode assumes thermionic emission over a voltage independent potential barrier. The current dependence on applied voltage takes on the simple exponential form

$$I_D = I_T = I_S\left[\exp\left(\frac{qV_D}{kT}\right) - 1\right] , \tag{2}$$

where

$$I_S = SA^*T^2 \exp\left(\frac{-\Phi_B}{kT}\right). \tag{3}$$

Here I_D is the current through the metal–semiconductor junction and V_D is the voltage drop across the junction. For the ideal diode, I_D equals the total current I_T and V_D equals the total applied bias V. The contact area is S, A^* is the effective Richardson constant, and q,k,T are the elementary charge, Boltzman constant, and absolute temperature, respectively.

In a nonideal diode, the I–V characteristic deviates from the simple expression (2). Linear and nonlinear leakages, barrier height dependence on voltage, recombination in the space charge region, tunneling across the potential barrier, and carrier trapping by interface states modify the nature of the carrier transport.[2] An ideality factor, $\beta \geqslant 1$, is commonly used to phenomenologically model the effect all the nonidealities ($\beta = 1$ for pure thermionic emission). In addition, part of the applied voltage drops across a series resistance stemming from the bulk semiconductor and the metal–semiconductor contact. The series resistance may include linear and nonlinear components. The result is a modification of the junction voltage drop so that $V_D = V - I_T R_S - A_0 I_T^{1/n}$. If $qV_D \gg \beta kT$, or $I_D \gg I_S$, the total applied voltage is related to the current I_T by

$$V = \frac{\beta kT}{q}\ln\left(\frac{I_T}{I_S}\right) + A_0 I_T^{1/n} + I_T R_S . \tag{4}$$

Equation (4) describes also *p-n* and *p-i-n* junctions with only the saturation current taking a form different from Eq. (3).[2] The nonlinear term in Eq. (4) results from one of several possible mechanisms.[11,15–17] Any nonlinear contribution ($n > 1$, $A_0 \neq 0$) in an ideal Schottky barrier diode is related to double carrier injection into the semiconductor at high forward voltages which yields $n = 2$.[15] A nonlinear current flow with a similar dependence on voltage takes place due to a carrier drift into the intrinsic region of ideal *p-i-n* diodes,[11,15] while carrier recombination in the intrinsic layer and the highly doped region near the back contact leads to an $n = 4$ dependence.[11,17] The coefficient A_0 is defined in Refs. 11,15–17 and depends on the type of carrier injection process in the high bias regime. The value of A_0 is determined by the densities, mobilities, diffusion constant, and diffusion length of thermally generated and excess injected carriers as well as the temperature. Experimental proofs of high voltage nonlinearity in the I–V characteristics of *p-i-n* diodes based on GaAsP and GaAlAs as well as in GaN *m-i-n* and porous silicon light-emitting diodes are described in Refs. 11, 13, 17, and 18.

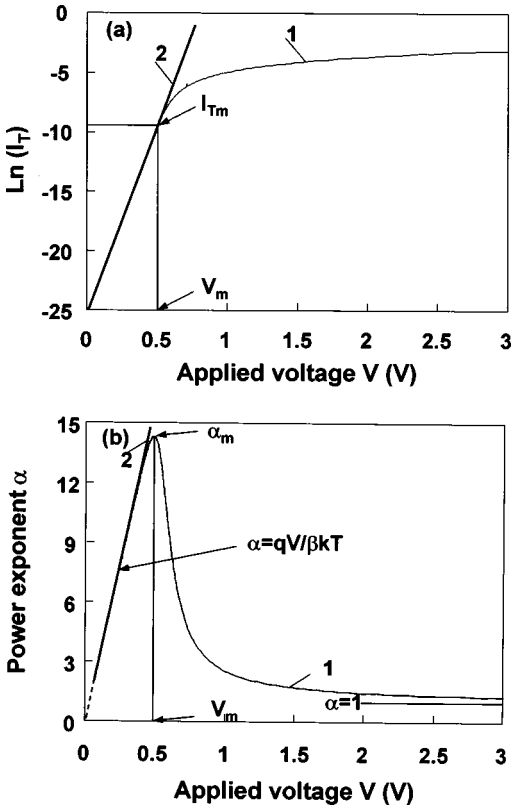

FIG. 1. Calculated (a) I–V and (b) α–V characteristics of a Schottky diode with (curve 1) and without (curve 2) series resistance: $R_S = 50\ \Omega$; $\beta = 1.25$; $\Phi_B = 0.88$ eV, $A^* = 112$ A/cm^2 K^2; $T = 293$ K; $S = 0.0016$ cm^2.

III. THE POWER EXPONENT METHOD

This section describes the use of the power exponent parameter, α, defined in Eq, (1), for a detailed analysis of the I–V characteristics of a nonideal Schottky barrier diode. A nonideal diode is simulated and the versatility of the α parameter is demonstrated by the ease with which the diode parameters are extracted.

A. Leakage free conduction

A calculated I–V curve of a Schottky Barrier diode containing a series resistance, no shunt leakage path ($I_T = I_D$) and no nonlinearity is plotted logarithmically in Fig. 1(a). The transition from low bias conditions where $V_D \gg I_D R_S$ to the regime, where the voltage drop $I_D R_S$ has a measurable effect is not easy to identify accurately. The α parameter calculated from Eq. (4) (with $A_0 = 0$) takes the form:

$$\alpha = \frac{qV}{\beta kT + qI_T R_S} \tag{5}$$

and is plotted in Fig. 1(b) as a function of V. At low bias, the α–V curve increases linearly reaching a maximum α_m before decreasing towards and stabilizing on a level of $\alpha = 1$. At low bias levels, the influence of the series resistance is

relatively insignificant. The degree of linearity of the low bias portion of the curve is a measure of the bias independence of β and of I_S (or Φ_B). The bias point I_{T_m} and V_m for which $\alpha=\alpha_m$ marks the point above which R_S has a large effect. In the regime where $\alpha=1$, the behavior is Ohmic since the voltage drop across R_S dominates.

1. First parameter extraction method: The use of α_m

The calculated α for the leakage free diode which contains linear and nonlinear current components at high bias levels is in accordance with Eq. (4):

$$\alpha=\frac{qV}{\beta kT+q[I_TR_S+(A_0/n)I_T^{1/n}]}. \tag{6}$$

The values of α_m, I_{T_m}, and V_m are easily found by differentiating Eq. (6) and setting $d\alpha/dV=0$. They are uniquely related to the physical parameters of the diode:

$$\beta=\frac{qV_m}{kT}\left[\frac{\alpha_m-n}{\alpha_m^2}+(n-1)\frac{I_{T_m}R_S}{V_m}\right], \tag{7a}$$

$$A_0=\frac{V_mn^2}{\alpha_m^2I_{T_m}^{1/n}}\left(1-R_S\alpha_m^2\frac{I_{T_m}}{V_m}\right), \tag{7b}$$

$$I_S=I_{T_m}\exp\left\{-(\alpha_m+n)\times\frac{1+[\alpha_m^2(n^2-1)I_{T_m}R_S)]/[(\alpha_m^2-n^2)V_m]}{1+[\alpha_m^2(n^2-1)I_{T_m}R_S)]/[(\alpha_m-n)V_m]}\right\}. \tag{7c}$$

Equations (7) can be used to extract the physical parameters of the diode provided that the value of n and at least one of the four parameters R_S, A_0, I_S (or Φ_B), and β are known.

In the simple case where the high bias portion of the I–V characteristics is strictly linear: $A_0=0, n=1, R_S\neq 0$, the relationships (7) become

$$\beta=\frac{qV_m(\alpha_m-1)}{kT\alpha_m^2}, \tag{8a}$$

$$R_S=\frac{V_m}{I_{T_m}\alpha_m^2}, \tag{8b}$$

$$I_S=I_{T_m}\exp[-(\alpha_m+1)],\ \text{or}\qquad \Phi_B=kT\left[(\alpha_m+1)-\ln\left(\frac{I_{T_m}}{ST^2A^*}\right)\right]. \tag{8c}$$

The second simple case is a high bias region in which the linear contribution to the current is negligible compared with the nonlinear component: $A_0\neq 0, n>1, R_S=0$. The relationships (7) now become

$$\beta=\frac{qV_m(\alpha_m-n)}{kT\alpha_m^2}, \tag{9a}$$

$$A_0=\frac{n^2V_m}{\alpha_m^2I_{T_m}^{1/n}}, \tag{9b}$$

$$I_S=I_{T_m}\exp[-(\alpha_m+n)],\ \text{or}\qquad \Phi_B=kT\left[(\alpha_m+n)-\ln\left(\frac{I_{T_m}}{ST^2A^*}\right)\right]. \tag{9c}$$

2. Second parameter extraction method: The use of α derivatives

The α–V characteristic of diodes which contains a finite R_S and a measurable nonlinearity does not exhibit a clear maximum point. A similar problem occurs in diodes with low barrier heights. Accurate parameter extraction requires in these cases additional manipulation of the I–V and α–V curves. We define the parameters:

$$\gamma=\frac{d(\ln\alpha)}{d(\ln V)}, \tag{10}$$

$$\Lambda=\frac{d(\ln\gamma)}{d(\ln V)}. \tag{11}$$

Using Eqs. (4) and (6), γ and Λ become

$$\gamma=1-\left(\frac{\alpha}{n}\right)^2\frac{n^2I_TR_S+A_0I_T^{1/n}}{V}, \tag{12}$$

$$\Lambda=\alpha^2\left[n^2I_TR_S(1-\alpha-2\gamma)-A_0I_T^{1/n}\left(1-\frac{\alpha}{n}-2\gamma\right)\right]. \tag{13}$$

The parameters γ and Λ are high order derivatives of the I–V curve. In order to avoid errors in the analyzing experimental data, we use a fast Fourier transform routine coupled with numerical digital filtering to smooth unrealistically sharp transitions which could otherwise cause computational errors. Assuming n is known (and is larger than one), the parameters R_S and A_0 are found to be

$$R_S=\frac{nV}{I\alpha^3(n-1)}\left[(1-\gamma)\left(1-2\gamma-\frac{\alpha}{n}\right)-\gamma\Lambda\right], \tag{14}$$

$$A_0=\frac{n^2V(1-\gamma)}{\alpha^2I_T^{1/n}}\left\{1+\frac{n}{\alpha(n-1)}\left[\frac{\Lambda\gamma}{1-\gamma}+2\gamma+\alpha-1\right]\right\}. \tag{15}$$

Using the more accurate formalism, we can again find, in the strictly linear case, the ideality factor β, together with R_S:

$$\beta=\frac{qV(\alpha-1)}{kT\alpha^2}\left(1+\frac{\gamma}{\alpha-1}\right),\quad R_S=\frac{V(1-\gamma)}{I_T\alpha^2}, \tag{16}$$

and in the nonlinear case with a negligible R_S, we get

$$\beta=\frac{qV(\alpha-n)}{kT\alpha^2}\left(1+\frac{\gamma n}{\alpha-n}\right),\quad A_0=\frac{n^2(1-\gamma)V}{\alpha^2I_T^{1/n}}. \tag{17}$$

The saturation current (and therefore the barrier height) may be determined using Eqs. (4), (6), or (7), just as in the case where α_m is clearly identified. The parameters resulting from

Eqs. (16) and (17) depend on bias. If the same values are obtained for a wide range of bias levels, the parameters are accurate.

3. Establishment of current flow mechanism at high bias levels

Accurate parameter extraction requires the determination of the carrier transport mechanism in the high bias regime which renders the value of n. Under the assumption of bias independent n and series resistance, $(dn/dV)=(dR_S/dV)=0$, we obtain n from Eq. (14)

$$n=\frac{\alpha}{1-2\gamma}\left\{\frac{1+\dfrac{\gamma(1-\gamma)}{(1-3\gamma-\alpha)(1-\gamma)-\gamma\Lambda}}{1-\dfrac{\gamma\Lambda}{1-2\gamma}\left[\dfrac{3+\Lambda+Q-5\gamma-\alpha}{(1-3\gamma-\alpha)(1-\gamma)-\gamma\Lambda}\right]}\right\}, \tag{18}$$

$$Q=\frac{d(\ln\Lambda)}{d(\ln V)}.$$

In the cases where the high bias current is dominated by the nonlinear contribution, we set $R_S=0$ and the value of n becomes according to Eq. (15)

$$n=\frac{\alpha}{1-2\gamma}\left\{\frac{1}{1-\gamma\Lambda/[(1-2\gamma)(1-\gamma)]}\right\}. \tag{19}$$

Equations (18) and (19) yield, for the respective conditions, a correct value of n throughout the complete range of applied bias, except for a narrow interval in the vicinity of α_m (where $d\alpha/dV=0$ and therefore γ,Λ, and $Q=0$). Once n is established, the values of R_S, A_0, and β are obtained. If these values are bias independent, we may conclude that their values are accurate and that the preassumed transport mechanism is correct.

B. The addition of a leakage conductance

Practical diodes contain a leakage conductance $G_L=1/R_P$ which shunts a fraction of the diode current. Figure 2(a) shows a calculated $\ln I$–V curve for bias independent G_L and R_S. The leakage conductance affects the characteristic in all bias regimes but its influence is easier traced in the α–V plot shown in Fig. 2(b). It modifies the low bias region adding a portion where $\alpha=1$. It also narrows the α–V characteristic and reduces the value of α_m. The α_m value, which is a strong function of the barrier height is plotted in Fig. 3 as a function of G_L for high (0.88 eV) and low (0.55 eV) barrier heights. We note that a small leakage has a negligible effect on α_m and hence on the extracted physical parameters. The influence of G_L increases as Φ_B rises consistent with Ref. 8.

The leakage conductance G_L is accounted for in the model by substituting in the I–V curve the expression for the diode current $I_D=I_T-G_LV_D$ and recalculating the α–V plot. This yields new values for α_m, I_{T_m}, and V_m which are used in conjunction with Eqs. (8) and (9) to extract the diode parameters R_S, β, I_S, and Φ_B, as in the leakage free case.

Conventional forward bias I–V characteristics [for example, Fig. 2(a), curves 1,2] are not suitable for the determination of the nature and magnitude of the leakage conductance. Instead, graphical treatments of the linear portion of reverse biased I–V curve are commonly used to extract G_L as described in Ref. 5. The need for reverse bias characterization complicates the measurement. Above and beyond that, the observation of a linear reverse current dependence on V does not yield unequivocally the nature of the leakage mechanism since the linear behavior may not result from a parallel leakage conductance but rather be from its thermionic emission, described in Ref. 19.

The distinctive feature of the low bias portion of the $\alpha-V$ curve, characterized by a constant α equal to unity in the case of an Ohmic parallel conductance [see Fig. 2(b),

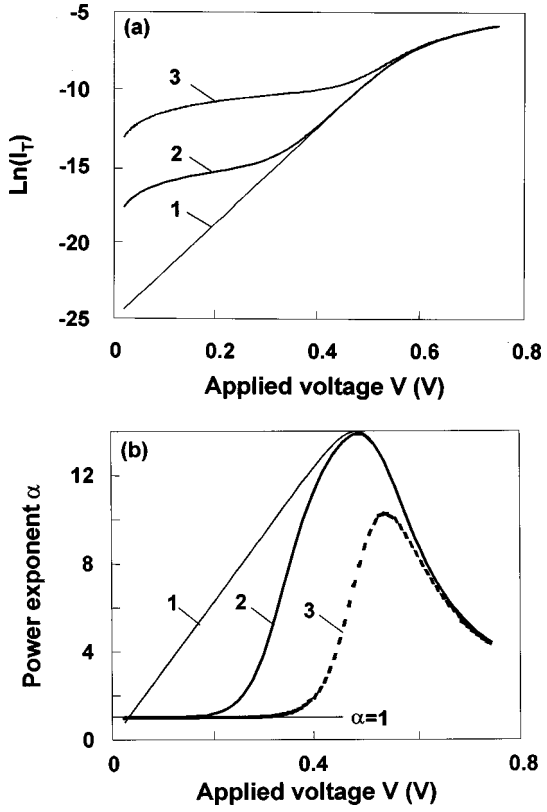

FIG. 2. Calculated (a) I–V and (b) α–V characteristics with parallel and series resistance: (1) $G_L=0$, (2) $G_L=1\times10^{-6}$, (3) $G_L=1\times10^{-4}\ \Omega^{-1}$ and $R_S=50\ \Omega$. $\beta=1.25$; $\Phi_B=0.88$ eV; $T=293$ K; $A^*=112\text{A/cm}^2\text{K}^2$; $S=0.0016\ \text{cm}^2$.

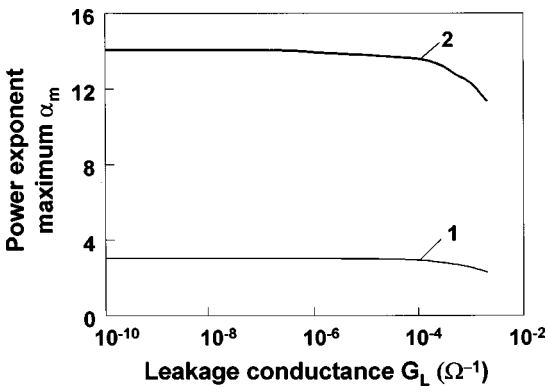

FIG. 3. α_m dependence on G_L. (1) $\Phi_B=0.55$ eV and (2) $\Phi_B=0.88$ eV. $\beta=1.25$; $R_S=50\ \Omega$; $A^*=112\text{A/cm}^2\text{K}^2$; $T=293$ K; $S=0.0016\ \text{cm}^2$.

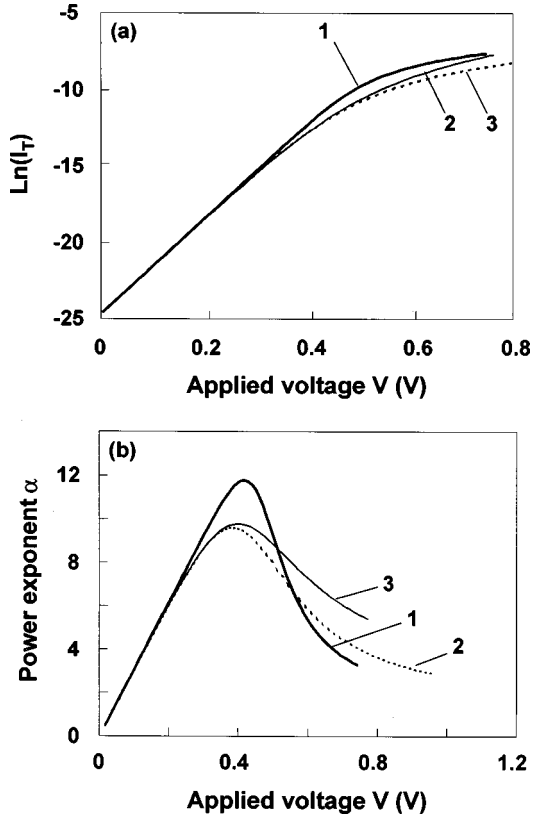

FIG. 4. Calculated (a) $I-V$ and (b) $\alpha-V$ characteristics with linear (curves 1), linear and nonlinear (curves 2), and nonlinear (curves 3) series resistances. (1) $A_0=0$, $R_S=400\ \Omega$; (2) $A_0=10\ \mathrm{A/V^{1/2}}$, $R_S=400\ \Omega$; (3) $A_0=10\ \mathrm{A/V^{1/2}}$, $R_S=0$. $\beta=1.285$; $n=2$; $\Phi_B=0.88$ eV; $A^*=112\ \mathrm{A/cm^2\,K^2}$; $T=293$ K; $S=0.0016\ \mathrm{cm^2}$.

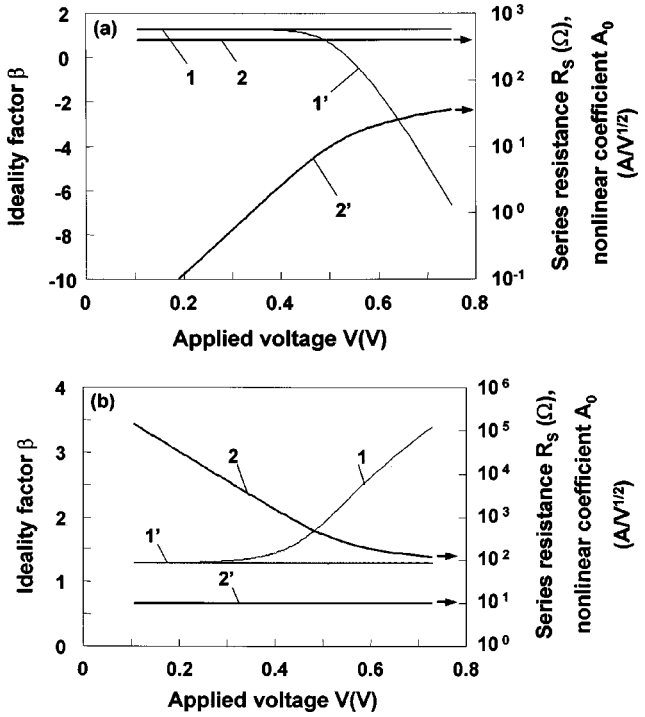

FIG. 5. Dependencies of calculated values of β [curves 1 and 1′, Eqs. (16) and (17)], R_S [curve 2, Eq. (16)], and A_0 [curve 2′, Eq. (17)] on applied voltage. (a) Linear and (b) nonlinear cases (see Figs. 4(a), 4(b), curves 1 and 3, respectively).

curve 3], may be used to reveal the leakage mechanism. Once the bias regime over which the leakage is linear ($\alpha=1$ and $G_L=dI_T/dV$ remains constant) is established, G_L is found easily. The result enables, in principle, to automatically (in contrast with Ref. 5, where the G_L from reverse $I-V$ is determined) correct for the leakage in the forward $I-V$ curve and to recover the intrinsic characteristics of the Schottky barrier.

The addition of G_L changes α_m, I_{T_m}, and V_m (see Fig. 2, curves 1,2) and hence the extracted device parameters. The values of α, I, and V are less sensitive to the value of G_L in the bias regime $V>V_m$ (see Fig. 2, curves 2 and 3) and therefore these extracted parameters are more reliable in comparison with those obtained from α_m.

IV. THE VALIDITY OF THE POWER EXPONENT METHOD

A. The influence of the high voltage nonlinearity

The validity of the method is demonstrated by a simulation of $I-V$ and $\alpha-V$ curves for given parameters, as shown in Fig. 4. Three cases are shown: Curve 1 describes the case of $R_S=400\ \Omega$, $A_0=10(\mathrm{A/V})^{1/2}$) and $n=2$. Curve 2 is the strictly linear case with $R_S=400\,\Omega$ and curve 3 represents the nonlinear case, $R_S=0$, $A_0=10(\mathrm{A/V^{1/2}})$, and $n=2$. A determination of n using Eqs. (18) and (19) and its invariability with applied voltage provides the required discrimination between the various current flow mechanisms in the cases we consider. In Fig. 5 we show the application of Eqs. (16) and (17) to obtain β, R_S, and A_0 from the simulated data of Fig. 4, curves 1 and 3. We note that the use of the correct equations yields bias independent parameters, as seen in Fig. 5(a) curves 1, 2, for the strictly linear case ($A_0=0$) and in Fig. 5(b) curves 1′, 2′ for the case where $R_S=0$ and $A_0\neq 0$. The values of the extracted parameters coincide with results obtained for the correct n values in accordance with Eqs. (7) to (9).

For comparison, we calculate and show in Fig. 6 the Werner plots[5] corresponding to the data of Fig. 4(a). We choose to use the Werner's method as a reference for comparison as it is widely accepted[8,9] as the most reliable of the published numerical methods. An obligatory condition of the validity of the Werner method is a linear G/I_D-G behavior, with $G=dI_D/dV$ being the differential conductivity. We note that the curves are linear only for the $A_0=0$ case. This fact demonstrates a basic problem of the Werner technique when the current flow mechanism in the high bias range becomes nonlinear.

B. The Limitation due to series resistance, barrier height, and voltage

The permissible range of applicability of all published Schottky diode parameters extraction methods[8] is limited by series resistance and barrier height values. These determine the bias intervals where the $I-V$ data remains linear in a semilogarithmic scale.

The low bias limit is set by the condition $V_D>3kT/q$ (0.08 V at $T=293$ K) which implies that the low bias portion

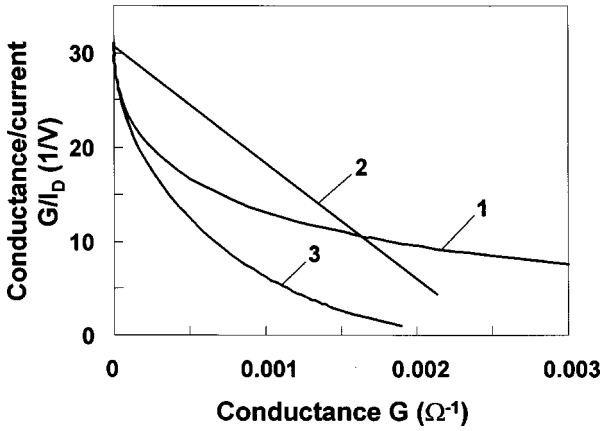

FIG. 6. Werner plots in accordance with I–V data of Fig. 4(a). (1) $R_S=0$, $A_0=10$ A/V$^{1/2}$; (2) $R_S=400\ \Omega$, $A_0=0$; (3) $R_S=400\ \Omega$, $A_0=10$ A/V$^{1/2}$.

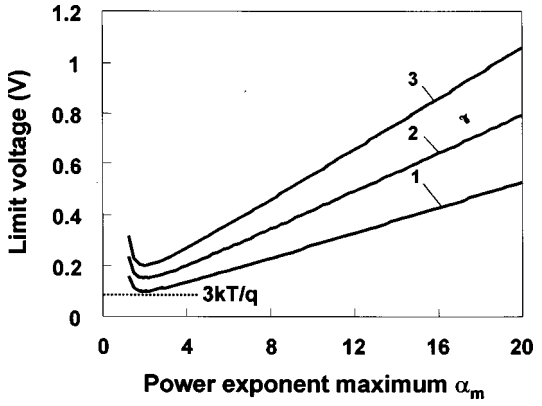

FIG. 8. V_m vs α_m, calculated for different values of ideality factor [Eq. (21)]. (1) $\beta=1$; (2) $\beta=1.5$, and (3) $\beta=2$.

of an I–V curve cannot be used as it does not follow the exponential law. The upper limit is set by a maximum series resistance R_{S_m} such that $R_{S_m}I_D \sim V_D/100$ which ensures that at high bias the $\ln I$–V curve is linear. This linearity is needed for the graphical parameter extraction techniques.[1–9]

The technique we propose here introduces new limiting conditions. Assuming that the method is correct at any value of α_m (or α) larger than unity and for bias levels larger than V_m, that is, provided that the conditions: $\alpha_m>1$ and $\beta kT/q<V_m$, hold, the limiting dependencies of the maximum series resistance and voltage on the barrier height are

$$R_{S_m}=\frac{k\beta\exp(\Phi_B/kT)}{A^*ST(\alpha_m-1)\exp(\alpha_m+1)}, \tag{20}$$

$$V_m=kT\beta\frac{\alpha_m^2}{(\alpha_m-1)}. \tag{21}$$

Figures 7, 8, and 9 show the interdependencies of R_{S_m}, V_m, α_m, and Φ_B, under the condition of $\alpha_m\geqslant 1.5$ (which is stronger than $\alpha_m\geqslant 1$) using simulated I–V characteristics of a diode having parameters taken from Ref. 8: $\beta=1$, $S=0.00384$ cm^2, $A^*=112$ A/cm^2 K^2 and $A_0=G_L=0$.

The advantage of the technique we propose is obvious when comparing Fig. 7 with results obtained using the graphical methods.[8] For room temperature [Fig. 7(a)] and a barrier height of $\Phi_B=0.6$ eV, the proposed method may be used up to $R_{S_m}=2500\ \Omega$ [see Fig. 7(a), curve 1], while for the conventional semilogarithmic and the Werner techniques, the maximum permissible value of R_{S_m} does not exceed 5 and 250 Ω, respectively. A further decrease of the barrier height causes an expected reduction of R_{S_m} but at $\Phi_B=0.5$

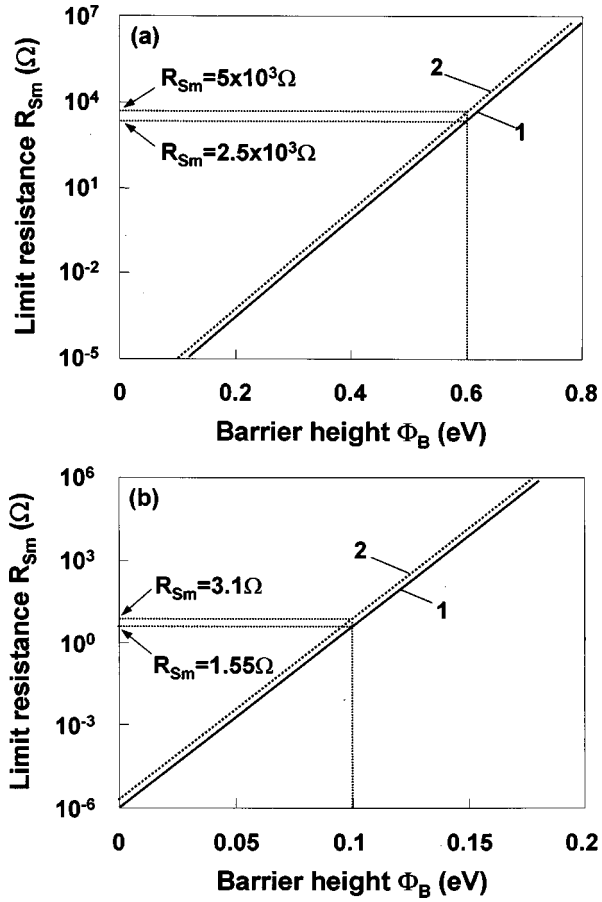

FIG. 7. Limit values of the series resistance R_{Sm} vs barrier height. $S=0.00384$ cm^2 $A^*=112$A/cm^2 K^2 (1) $\alpha_m=1.5$, $\beta=1$; (2) $\alpha_m=1.5$, $\beta=2$. (a) 293 K, (b) 77 K.

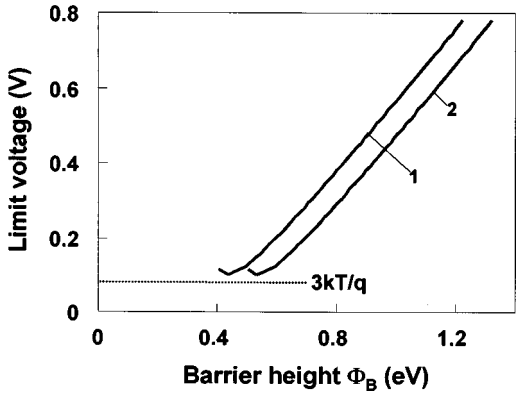

FIG. 9. V_m vs barrier height, calculated for different quantities of the R_S [Eq. (20)]. (1) $R_S=1\ \Omega$ and (2) $R_S=50\ \Omega$. $\alpha_m=1.5$; $\beta=1$; $T=293$ K; $A^*=112$ A/cm^2 K^2; $S=0.00384$ cm^2.

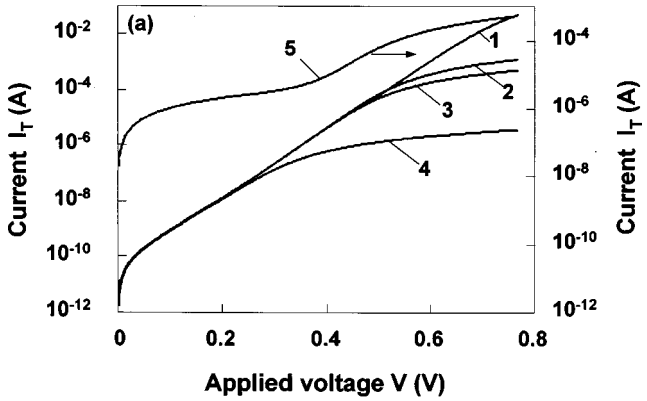

FIG. 10. Experimental (a) $I-V$ and (b) $\alpha-V$ characteristics of a commercial Si Schottky diode, measured with and without additional series and parallel linear resistances. (1) without additional resistances; (2) with additional resistances in series: $R_S=130\,\Omega$; (3) $R_S=400\,\Omega$; (4) $R_S=1\times10^5\,\Omega$; (5) with added resistances in series and in parallel: $R_S=400$ and $R_P=1\times10^5\,\Omega$.

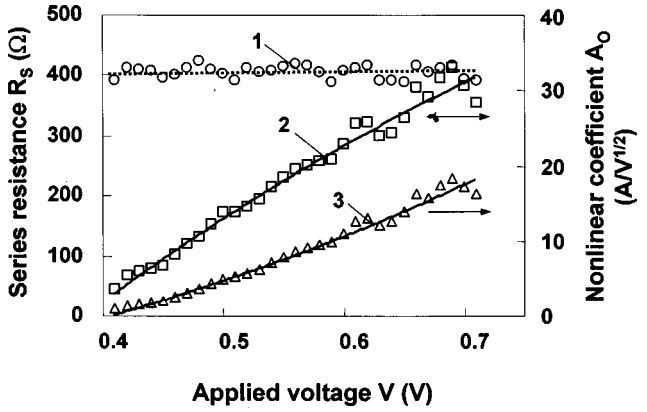

FIG. 11. Voltage dependencies of R_S and A_0 in the Si Schottky diode. At the high voltage region, the $I-V$ is approximated by $V\sim IR_S$ (curve 1) or $V\sim A_0I^{1/n}$ (curves 2, $n=2$ and 3, $n=4$). The values of R_S and A_0 are obtained, respectively, by Eqs. (14) and (15).

eV, it is still fairly large ($R_{S_m}=50\,\Omega$) compared with $\sim10\,\Omega$.[8] At low temperatures, R_{Sm} increases for all barrier heights [see Fig. 7(b)] and there is almost no limitation to the proposed technique for practical values of the series resistance.

Calculated room temperature $V_m-\alpha_m$ and $V_m-\Phi_B$ curves based on Eqs. (20) and (21) are shown in Fig. 8 and Fig. 9 for various values of ideality factor and series resistance. We note that the limitation of V_m is completely determined by α_m and its smallest value [consequence of $\alpha_m=1.5$ and $\beta=1$ (Fig. 8, curve 1)] always satisfies the condition $V_m>\beta kT/q$ (which is, as was noted above, the lower bias limit). Thus, independent of the value of R_{S_m}, if $\alpha_m\geqslant1.5$ is a correct condition for the proposed method, it holds for any applied bias $V\geqslant V_m$ as seen in Fig. 9. Finally, we note that V_m depends linearly on β as stated in Eq. (21) and that low temperature operation reduces the minimum voltage for which the procedure holds.

V. EXPERIMENTAL VERIFICATION

We have applied our parameter extraction procedure to three kinds of Schottky diodes based on Si, InGaP, and HgCdTe as well as to an InGaAs/InGaAsP *p-n* junction of a multiple quantum well laser diode.

TABLE I. Physical parameters extracted from experimental data of the silicon Schottky diode (with and without added external resistors which simulate series and parallel resistances). In parenthesis we show extracted parameters using the Werner technique.[b]

Parameters Measurement conditions		Power exponent maximum, α_m	Voltage at maximum, V_m (V)	Current at maximum, I_m (A)	Series resistance, R_S (Ω)	Ideality factor, β	Saturation current, I_S (A)	Barrier height, Φ_B (eV)	Shunt resistance, R_P (Ω)
Additional resistance in series (Ω)	Additional resistance in parallel (Ω)								
0	0	17.2	0.63	3.0×10^{-3}	0.71 (1.5)	1.36 (1.35)	3.74×10^{-11} (4.25×10^{-11})	0.85 (0.85)	0
1.3×10^2	0	12.3	0.455	2.3×10^{-5}	1.31×10^2 (1.37×10^2)	1.35 (1.31)	3.85×10^{-11} (2.62×10^{-11})	0.85 (0.857)	0
4.0×10^2	0	11.7	0.425	7.9×10^{-6}	3.93×10^2 (4.13×10^2)	1.32 (1.31)	2.41×10^{-11} (2.58×10^{-11})	0.86 (0.84)	0
1.0×10^5	0	6.54	0.27	6.1×10^{-8}	1.035×10^5 (9.9×10^4)	1.39 (1.46)	3.24×10^{-11} (5.32×10^{-11})	0.853 (0.8456)	0
4.0×10^2	1.0×10^5	11.65[a]	0.421[a]	7.6×10^{-6}[a]	4.05×10^2 (4.07×10^2)	1.31 (1.31)	2.45×10^{-11} (2.66×10^{-11})	0.86 (0.8631)	1.044×10^5

[a]After separation of leakage current from total.
[b]See Ref. 5.

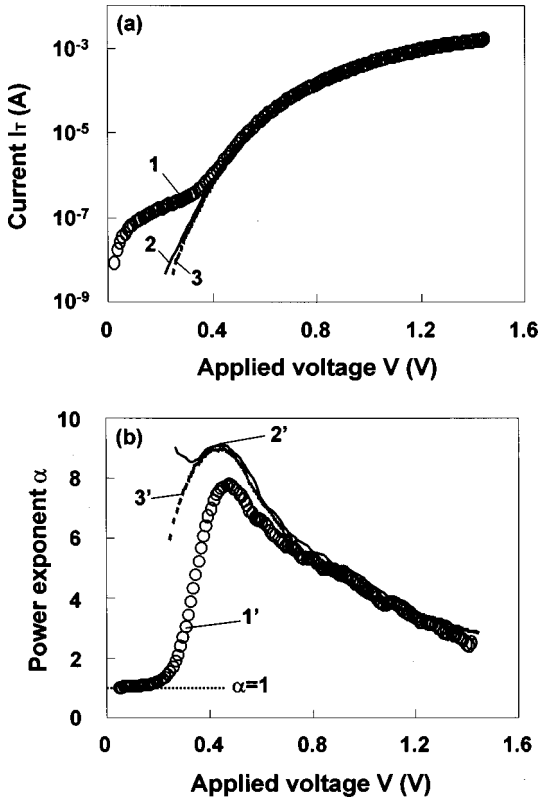

FIG. 12. Experimental (a) $I-V$ (curves 1, 2, 3) and (b) $\alpha-V$ (curves $1'$, $2'$, $3'$) characteristics of the Ti/Au–InGaP Schottky diode. (1, $1'$) as measured; (2, $2'$) after separation of the leakage component from the total current; (3, $3'$) calculated, based on Eqs. (14), (15), (7), and (18). $R_S=100\,\Omega$, $A_0=10.5$ A/V$^{1/2}$; $\beta=1.285$; $I_S=5.92\times10^{-12}$ A, and $n=2$.

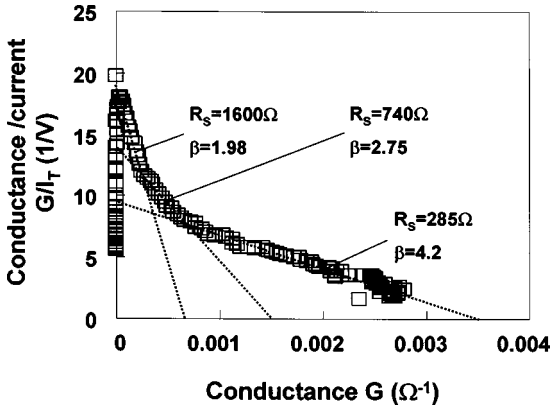

FIG. 14. Werner plot, obtained from data of the $I-V$ curve shown in Fig. 12 (curve 1). The parameters β and R_S are calculated, respectively, from the G/I_T and G axes intercepts by the linear (dashed) lines.

lower voltage due to series resistance are clearly seen. A linear dependence represented by $\alpha=1$ under low bias and the narrowing of the $\alpha-V$ curves as a result of a parallel resistance as well as the shrinking of the exponential part of $I-V$ are also observed.

The parameter n obtained from data of curve 3 in Fig. 10 [using Eq. (18)] is close to 1, independent of the series resistance (curve 1 in Fig. 11). In contrast A_0 shown in curves 2 and 3 of Fig. 11 varies significantly with bias. Therefore, we conclude that the conduction processes under high bias is only due to voltage independent series resistance.

A. Silicon based Schottky diodes

Experimental $I-V$ characteristics measured at room temperature for a commercial Silicon based Schottky diode and the corresponding $\alpha-V$ curves are shown in Fig. 10. In order to simulate parasitic elements as well as voltage drops other than that of the proper diode structure, we connected resistors of various values in series and in parallel with the diode.

All the typical features discussed in Sec. III are exhibited in Fig. 10, as expected. An $\alpha-V$ curve which shows a clear maximum, α_m, the reduction of α_m and its shift towards a

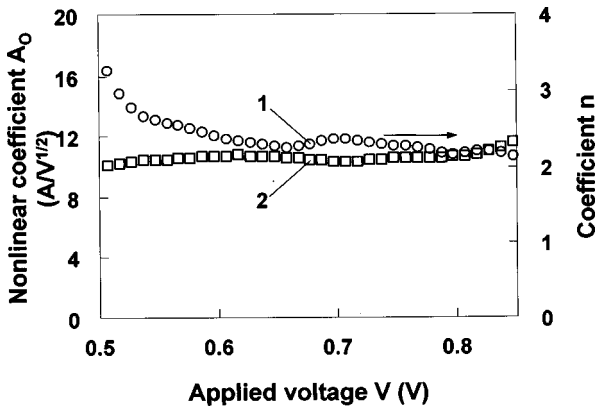

FIG. 13. Voltage dependencies of the n (curve 1) and A_0 (curve 2) for the Ti/Au–InGaP diode.

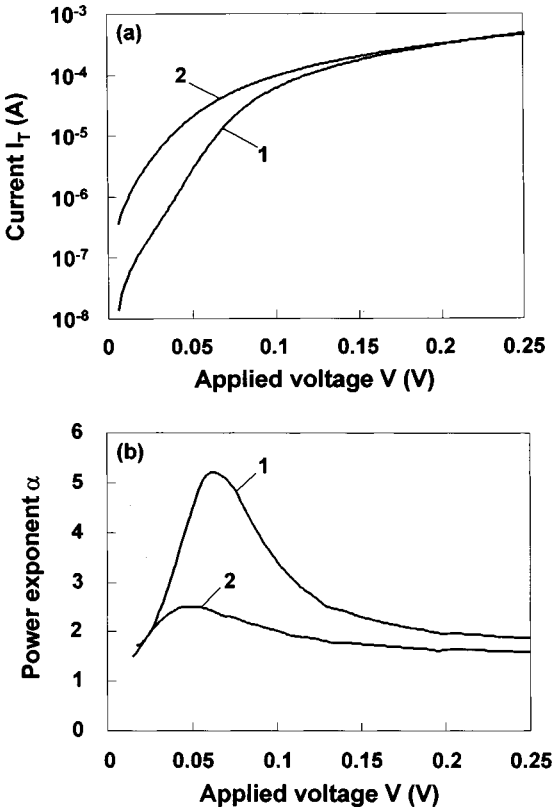

FIG. 15. Experimental (a) $I-V$ and (b) $\alpha-V$ characteristics of Ti/Au–CdHgTe structure. Curve 1, 75.3 K, curve 2, 115 K.

TABLE II. Physical parameters extracted from experimental data of the HgCdTe Schottky diode at 75.3 and at 115 K.

Parameters / Temperature (K)	Power exponent maximum, α_m	Voltage at maximum, V_m(V)	Current at maximum, I_m(A)	Series resistance, $R_S(\Omega)$	Ideality factor, β	Saturation current, I_S(A)	Barrier height Φ_B(eV)
75.3	5.21	0.057	4.9×10^{-6}	428	1.365	9.85×10^{-9}	0.102
115	2.5	0.045	1.48×10^{-5}	485	1.092	4.52×10^{-7}	0.126

The α_m, I_{T_m}, V_m values obtained for the different cases and the calculated quantities of β, R_S, I_S, and Φ_B in accordance with Eqs. (8), (9), and (16) are summarized in Table I with all parameters obtained from unsmoothed $I-V$ and $\alpha-V$ curves. Also stated in the table are results of Werner plots. The ideality factor and saturation current (and therefore the barrier height) for the different series resistors do not differ much from the case of the diode alone. The maximum percentage deviations of parameters are 5, 3.5, and 1.5, respectively, for β, R_S, and Φ_B. The data shown in the fifth row of Table I reflect results corresponding to curve 5 of Fig. 10(a), processed in accordance with the expression: $I_D=I_T-G_LV$. The value of the parallel conductance was determined from the low bias portion [$\alpha=1$, see curve 5 of Fig. 10(b)] of the $I-V$ characteristic. A parallel resistance of $1\times10^5\,\Omega$ has only a minor influence on the accuracy of the obtained parameters. The results obtained from the Werner method are very similar for all resistor values.

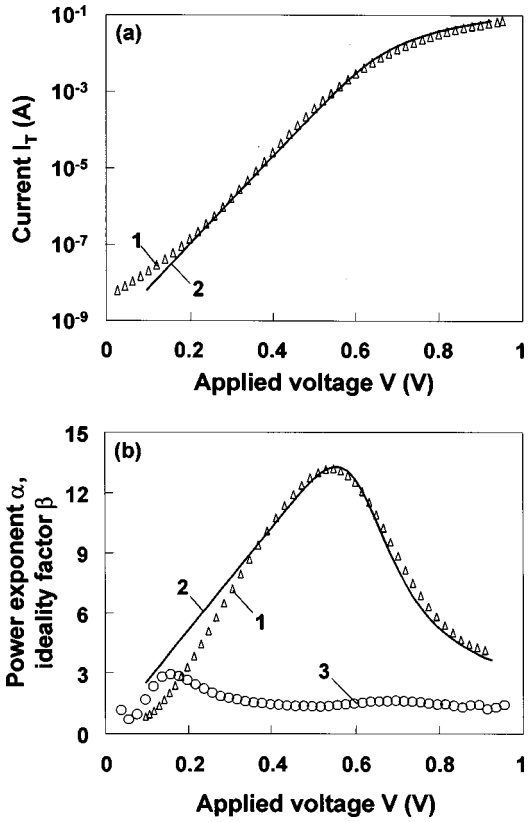

FIG. 16. (a) $I-V$, $\alpha-V$ and (b) $\beta-V$ dependencies of InGaAs/InGaAsP *p-n* multiple quantum well laser diode. Curves 1 and 2 show, respectively, experimental and calculated data; Curve 3 in (b) shows the $\beta-V$ characteristic.

B. InGaP based Schottky diodes

The experimental $I-V$ and $\alpha-V$ curves for a InGaP/InP Schottky diode are shown in Fig. 12. The metalorganic chemical vapor deposition (MOCVD) grown $In_{0.8}Ga_{0.2}P$ had an *n*-type background concentration of $10^{15}-10^{16}\,cm^{-3}$. The metal contact was Ti/Au with an area of $S=0.025\,cm^2$ and was not annealed. The Richardson constant is $A^*=8\,A/cm^2\,K^2$,[2] and the diode was characterized at $T=293$ K. This diode exhibits a linear leakage ($G_L=8.6\times10^{-7}\,\Omega^{-1}$) with $\alpha=1$ up to a voltage of 0.22 V (see curve 1′). The separation of the leakage component from the total current modifies the low bias characteristics and consequently α_m, I_{T_m}, and V_m with the change in I_{T_m} being the largest (see respectively, curves 1,1′ and 2,2′ of Fig. 12). This changes the series resistance we determine in comparison with the value calculated from the low bias $I-V$ and $\alpha-V$ characteristics (curves 1, 1′). Note that the slight drop in Fig. 12(b) curve 2 is an artifact of the digital smoothing procedure.

To establish a current flow mechanism in the high bias region, we determine the voltage dependence of *n* in accordance with Eq. (18). The value of *n* is approximately constant, $n=2.2$ to 2.5 (Fig. 13, curve 1). The deviation of the $I-V$ characteristic from the exponential law is due to a simultaneous linear and nonlinear current flow mechanism. Curves 3 and 3′ of Fig. 12, calculated in accordance with the determined values of *n* and with $A_0=10.5\,A/V^{1/2}$, $\beta=1.285$, $R_S=100\,\Omega$, $I_S=5.92\times10^{-12}$ A ($\Phi_B=0.89$ eV) show good agreement with the experimental (separated) $I-V$ and $\alpha-V$ characteristics (curves 2 and 2′ of Fig. 12).

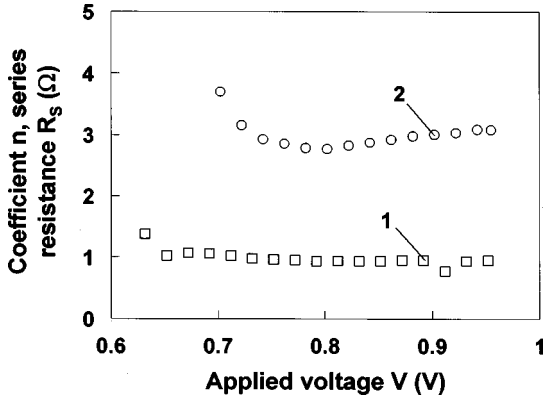

FIG. 17. Nonlinearity coefficient *n* (curve 1) and series resistance R_S (curve 2) vs applied bias in the InGaAs/InGaAsP *p-n* multiple quantum well laser diode.

The Werner model plot, shown in Fig. 14, needs to be approximated by a single linear curve. There are at least three such regions, yielding different values of β (2–4.2) and R_S (285–1600 Ω). We conclude that unlike in the linear Si diode, the nonlinear InGaP diode cannot be analyzed properly by the Werner method, while our proposed technique results in good agreement with the experimental data.

C. HgCdTe based Schottky diodes

The use of our parameter extraction technique in conjunction with low-band-gap diodes is demonstrated using Ti/Au–HgCdTe Schottky diodes operating at low temperatures. The composition of the liquid phase epitaxy (LPE) grown *p*-type semiconductor was $Hg_{0.78}Cd_{0.22}Te$, its doping level was 7×10^{15} and the metal contact was not annealed. Figure 15 shows I–V and α–V curves measured at 75.3 K (curve 1) and 115 K (curve 2). As the exponential part of the I–V curve shrinks with temperature, the use of conventional methods becomes difficult. The α–V curves are also sensitive to temperature but as long as the maximum point is clearly observable, exact parameter extraction is easy. This is related to the increase of R_{Sm} at low temperatures as seen in Fig. 7(b). Taking into consideration the values of the Richardson coefficient for CdHgTe $A^*=72\text{A/cm}^2\,\text{K}^2$ (Ref. 20) and the contact area of these diodes $S=1.6\times10^{-7}$ cm^2, for $\Phi_B=0.1$ eV and $\beta=1$, we get $R_{Sm}=1.45\times10^5\,\Omega$ and $R_{Sm}=4.2\times10^2\,\Omega$ for 75 and 115 K, respectively [see Eq. (20)]. The extracted physical parameters of the Ti/Au–HgCdTe Schottky diodes are listed in Table II.

D. *p-n* junction of a InGaAs/InGaAsP multiple quantum well diode lasers

In order to demonstrate the use of our parameter extraction technique for analysis of a *p-n* diode, we examined an InGaAs/InGaAsP multiple quantum well laser diode whose measured I–V characteristic is shown in Fig. 16(a) (curve 1) together with a calculation (curve 2). Figure 16(b) shows the measured α–V (curve 1) which fits well to a corresponding calculated characteristic (curve 2). Both calculated curves made use of the extracted parameters $I_S=9.85\times10^{-11}$ A and $R_S=3\,\Omega$. The α–V curve has a rather standard form and does not show any ($\alpha=1$) linear leakage region. Also shown in Fig. 16(b) is a β–V curve.

Figure 17 shows the dependence on bias of n and R_S. The invariability of the value of n, which equals unity for all bias levels, means that the linear series resistance alone influences the current flow mechanism at large bias. The value of R_S is almost independent of bias (see curve 2 of Fig. 17).

The experimental and calculated I–V and α–V curves deviate in the low bias region where the tail on experimental I–V and α–V dependencies is observed and the linearity of the power exponent with voltage is disturbed. In this region, $\beta>2$ due to a possible nonlinear leakage such as tunneling. At larger voltages, β becomes almost independent of voltage meaning that a single current transport mechanism takes place. These results show the applicability of the suggested method to *p-n* diodes in the case of voltage independence parameters.

VI. DISCUSSION

In this article we have presented a new parameter extraction technique suitable for analysis of I–V curves of nonideal Schottky barrier *p-i-n* and *p-n* diodes whose parameters are bias independent. The technique makes use of the power exponent parameter α and its bias dependence. It accommodates linear and nonlinear series and shunt resistances and lends itself to easy automation. We have presented experimental confirmations using Si, InGaP, and HgCdTe based Schottky diodes as well as *p-n* diode based on an InGaAs/InGaAsP multiple quantum well laser structure. The experiments demonstrate the advantage of the new technique over other published methods, especially for diodes which exhibit nonlinear characteristics in the high voltage regime.

The limitation of bias independent parameters requires some discussion. References 9 and 10 offer a limited solution which not only are complex or incomplete, but leave out the key point of establishing the exact current flow mechanism and its relevant bias regimes. Adding measurements at several temperatures[21] can help but they further complicate the measuring procedure. The technique we propose, while assuming bias independent parameters, can nevertheless shed light on the qualitative form of the $\beta(V)$ behavior. As long as $d\beta/dV=0$, we can get from Eq. (6) the form of $\beta(V)$ but unlike in Ref. 10, our result would include the influence of linear and nonlinear resistances. Further, an examination of Eq. (6) at bias levels below α_m, renders a measure of the change in current flow mechanism which manifests itself in deviation from linearity of the curve. This is indeed seen in the experimental $\alpha(V)$ and $\beta(V)$ characteristics shown in Fig. 16(b). We conclude, however, that the bias dependence is of minor significance in most practical devices, at least for a measurable range of voltages. The present technique can be further developed to include a barrier height dependence on bias and the consequent dependence of all other parameters. This addition, which does not compromise the advantages described in this article, will be shown in a future publication.

[1] H. Norde, J. Appl. Phys. **50**, 5052 (1979).
[2] S. M. Sze, *Physics of Semiconductor Devices* (Wiley, New York, 1981).
[3] C. D. Lien, F. C. T. So, and M. A. Nicolet, IEEE Trans. Electron Devices **ED-31**, 1502 (1984).
[4] S. K. Cheung and N. W. Cheung, Appl. Phys. Lett. **49**, 85 (1986).
[5] J. H. Werner, Appl. Phys. A: Solids Surf. **47**, 291 (1988).
[6] T. C. Lee, S. Fung, C. D. Beiling, and H. L. Au, J. Appl. Phys. **72**, 4739 (1992).
[7] D. Gromov and V. Pugachevich, Appl. Phys. A: Solids Surf. **59**, 331 (1994).
[8] V. Aubry and F. Meyer, J. Appl. Phys. **76**, 7973 (1994).
[9] M. Lyakas, R. Zaharia, and M. Eizenberg, J. Appl. Phys. **78**, 5481 (1995).
[10] C. Popescu, J. C. Manifacier, and R. Ardebili, Phys. Status Solidi A **158**, 611 (1996).
[11] A. N. Zyuganov and S. V. Svechnikov, *Injection Contact Phenomena in Semiconductors* (Naukova Dumka, Kiev, 1981) (in Russian).
[12] G. D. Bagratishvili, R. B. Dzanelidze, D. A. Jishiashvili, L. V. Piskanovskii, A. N. Zyuganov, V. M. Mikhelashvili, and P. S. Smertenko, Phys. Status Solidi A **65**, 701 (1981).
[13] A. N. Zyuganov, V. V. Zorikov, M. S. Matinova, V. M. Mikhelashvili, and R. I. Chikovani, Sov. Tech. Phys. Lett. **7**, 493 (1981).
[14] V. Mikhelashvili, Y. Betzer, I. Prudnikov, M. Orenstein, D. Ritter, and G. Eisenstein, J. Appl. Phys. **84**, 6747 (1998).
[15] A. Rose, J. Appl. Phys. **35**, 2664 (1964).

[16] J. L. Wagener and A. G. Milnes, Solid-State Electron. **8**, 495 (1965).
[17] I. V. Rizhikov, V. P. Sushkov, P. I. Tepaikin, and I. L. Kasatkin, Phys. Status Solidi A **69**, 707 (1982).
[18] C. Peng, K. D. Hirschman, and P. M. Fauchet, J. Appl. Phys. **80**, 295 (1996).
[19] L. L. Chang, Solid-State Electron. **8**, 721 (1965).
[20] *Properties of Narrow Gap Cadmium-based Compounds*, edited by P. Capper (INSPEC, IEE, UK, 1994).
[21] D. Danoval, M. Barus, and M. Zdimal, Solid-State Electron. **32**, 961 (1989).